In vitro biomarker discovery in the parasitic flatworm Fasciola hepatica for monitoring chemotherapeutic treatment

Morphew, Russell Mark; MacKintosh, Neil Douglas; Hart, Elizabeth Helen; Prescott, Mark; LaCourse, E. James; Brophy, Peter Michael

Published in:
EuPA Open Proteomics

DOI:
10.1016/j.euprot.2014.02.013

Publication date:
2014

Citation for published version (APA):
Morphew, R. M., MacKintosh, N. D., Hart, E. H., Prescott, M., LaCourse, E. J., & Brophy, P. M. (2014). In vitro biomarker discovery in the parasitic flatworm Fasciola hepatica for monitoring chemotherapeutic treatment. *EuPA Open Proteomics*, *3*, 85-99. https://doi.org/10.1016/j.euprot.2014.02.013

Available online at www.sciencedirect.com

ScienceDirect

journal homepage: http://www.elsevier.com/locate/euprot

In vitro biomarker discovery in the parasitic flatworm *Fasciola hepatica* for monitoring chemotherapeutic treatment

Russell M. Morphew[a,*], *Neil MacKintosh*[a], *Elizabeth H. Hart*[a], *Mark Prescott*[b], *E. James LaCourse*[c], *Peter M. Brophy*[a]

[a] *Institute of Biological, Environmental and Rural Sciences (IBERS), Aberystwyth University, Aberystwyth, Ceredigion, Wales SY23 3DA, UK*

[b] *School of Biological Sciences, University of Liverpool, Liverpool, Merseyside, England, UK*

[c] *Liverpool School of Tropical Medicine, L3 5QA, UK*

ARTICLE INFO

Article history:
Received 16 December 2013
Received in revised form
30 January 2014
Accepted 28 February 2014
Available online 12 March 2014

Keywords:
Proteomics
Biomarkers
Triclabendazole
Calreticulin

ABSTRACT

The parasitic flatworm *Fasciola hepatica* is a global food security risk. With no vaccines, the sustainability of triclabendazole (TCBZ) is threatened by emerging resistance. *F. hepatica* excretory/secretory (ES) products can be detected in host faeces and used to estimate TCBZ success and failure. However, there are no faecal based molecular diagnostics dedicated to assessing drug failure or resistance to TCBZ in the field. Utilising *in vitro* maintenance and sub-proteomic approaches two TCBZ stress ES protein response fingerprints were identified: markers of non-killing and lethal doses. This study provides candidate protein/peptide biomarkers to validate for detection of TCBZ failure and resistance.

1. Introduction

The liver fluke, *Fasciola hepatica*, is an invasive parasitic trematode causing both acute and chronic disease. Liver fluke is a food security risk causing annual losses of more than US$3000 million to livestock production worldwide through livestock mortality and by decreased productivity *via* reduction of milk, wool and meat yields [1]. Further impacts on cattle productivity result from a negative association between the exposure to *F. hepatica* and the diagnosis of Bovine tuberculosis [2]. *F. hepatica* is also responsible for human food borne disease as an emerging worldwide zoonosis, with nearly 180 million people at risk [3]. In the absence of commercial vaccines, control of fascioliasis in livestock is mostly based on treatment with anthelmintic drugs. The current drug of choice for treatment of fascioliasis is triclabendazole (TCBZ), a benzimidazole-derivative, which shows activity against both pathogenic juvenile and mature flukes. TCBZ has been the mainstay of flukicides for *Fasciola* control for more than 20 years [4]. However, TCBZ control of *F. hepatica* may have been compromised

Abbreviations: TCBZ, triclabendazole; TCBZ-SO, triclabendazole sulphoxide; TCBZ-R, triclabendazole resistance; ES, excretory/secretory; Con, control dose of triclabendazole (0 μg/ml); SL, sub-lethal dose of triclabendazole (15 μg/ml); L, lethal dose of triclabendazole (50 μg/ml); CRT, calreticulin; Cat L, cathepsin L.

* *Corresponding author*. Tel.: +44 01970 621511; fax: +44 01970 622350.
E-mail address: rom@aber.ac.uk (R.M. Morphew).

http://dx.doi.org/10.1016/j.euprot.2014.02.013

with the apparent emergence of TCBZ resistance (TCBZ-R), first encountered in Australia [5] and since reported pan Europe [see 6]. Current suggested resistance levels may be exacerbated following the end of patent protection leading to generic forms of TCBZ for wider application and potential misuse. Furthermore, poor on-farm management of TCBZ dosing or poor host metabolism of TCBZ would mimic and ultimately simulate TCBZ resistance if parasites are exposed to sub-optimal drug levels. In addition, infection from the non-pathogenic but widespread rumen fluke also interferes with resistance monitoring of liver fluke; eggs are visually similar and generate false-positives on resistance testing by routine faecal egg count reduction tests. Thus, species specific markers for liver fluke following drug exposure are required for appropriate control [7].

There is a wealth of research dedicated to further understanding the mode of action of TCBZ but the multifaceted and highly complex mechanisms are yet to be resolved at the molecular level [8]. For example, laboratory reported effects of TCBZ on liver fluke include tegumental disruption through inhibition of tegumental secretory body movement [9–11], disruption of egg formation *via* mitotic inhibition of vitelline cells [12], apoptosis in the testes, ovary and vitelline follicles [13], inhibition of protein synthesis [14] and the stimulation of glucose-derived acetate and propionate [15]. Host and parasite biotransformation of TCBZ further complicate attempts to understand TCBZ mode of action [16]. TCBZ is, primarily oxidised by the host liver into the major active metabolite, triclabendazole sulphoxide (TCBZ-SO) *via* the flavin monooxygenase pathway and cytochrome P450 [17,18]. Further metabolism yields levels of triclabendazole sulphone (TCBZ-SO_2), a potent flukicide in its own right [9] and hydroxylated metabolites (OH-TCBZ, OH-TCBZ-SO and OH-TCBZ-SO_2) [19].

Our hypothesis is that, due to its multiple effects on parasite metabolism, TCBZ treatment will leave measurable protein signatures in the host environment when the parasite is successfully killed or the parasite is resistant to the drug or a sub-lethal drug failure is occurring. Previous antibody based studies have showed that liver fluke protein products survive the passage *via* host intestine and can subsequently be detected in host faeces [20]. Our previous proteomics studies also directly detected liver fluke proteins in host bile [21]. Therefore, proteomics supported by genomic/transcriptomic databases, in principle, can provide the detailed drug response information required to develop new field based tests.

Moreover, a current molecular test for indicating the presence of liver fluke infection operates on this basis *i.e.* the release of parasite proteins can be detected in host faeces (BioK antigen detection kit, BioX Diagnostics). Therefore, drug induced, released ES products will provide us with a suite of proteins specifically associated with successful or failed drug treatment that may be detectable in the host faeces. New approaches are needed to support liver fluke management, especially given the continued absence of commercial vaccines, apparent fluke resistance to TCBZ, interference by rumen fluke on monitoring liver fluke, no chemical treatments available for snail control, a limited opportunity to move livestock to un-parasitised land and the cost and limitations of drainage opportunities to remove a mobile aquatic intermediate stage.

Proteomics offers the opportunity to identify biomarker panels for monitoring anthelmintic efficiency in the field [22]. Therefore, we have taken a proteomic lead strategy to develop a biomarker panel for TCBZ-SO response in *F. hepatica*. We aimed to determine the protein complement released from adult *F. hepatica* during TCBZ-SO exposure which will potentially be shed from the host *via* the faeces. From this approach a potential set of biomarkers for assessing anthelmintic TCBZ/TCBZ-SO treatment will be generated and our understanding of the mode of action of TCBZ-SO could also be enhanced. We incorporate proteomics to delineate the excretory/secretory products of naturally infected adult *F. hepatica* released during *in vitro* maintenance under TCBZ-SO exposure using 2-DE, mass spectrometry and bioinformatics as a chemotherapy case study.

2. Materials and methods

2.1. *ES product collection: in vitro maintenance*

Live adult *F. hepatica* from natural infections were collected from the livers and bile ducts of newly slaughtered sheep at a local collaborating abattoir and immediately washed in PBS at 37 °C. Fluke were pooled and washed for 1 h with PBS replacement every 15 min. Post-washes, replicates of 10 adult, sized matched, worms were placed into fluke DME culture media containing 15 mM HEPES, 61 mM glucose, 2.2 mM Calcium acetate, 2.7 mM Magnesium sulphate, 1 μM serotonin and gentamycin (5 μg/ml) as previously described [23]. Maintenance cultures were allowed to incubate at 37 °C for 2 h (including transport to the proteomics laboratory) to establish a baseline protein profile. Upon completion of the initial 2 h incubation, culture media was replaced and supplemented with TCBZ-SO (LGC Standards, UK) at 50 μg/ml (lethal dose) or 15 μg/ml (sub-lethal dose) in DMSO (final conc. 0.1%, v/v). For control samples only DMSO was added to a final volume of 0.1% (v/v). Fluke maintenance cultures were allowed to incubate at 37 °C for a 6 h time period after which the media was refreshed, containing DMSO and TCBZ-SO at same concentration if required. Fluke maintenance cultures were allowed to incubate at 37 °C for a further 6 h. A final refreshment of culture media was conducted and fluke maintenance cultures allowed to incubate for an additional 12 h at 37 °C. Upon completion of the maintenance culture, fluke were removed from the media and snap frozen individually in liquid N_2. Protease inhibitors (CompleteMini, Roche, UK) were added to all media, after the allotted incubation, and immediately snap frozen in liquid N_2 prior to preparation for proteomic analysis. All samples were stored at −80 °C.

2.2. *Preparation and 2D proteomics*

Collected ES products from pooled samples were prepared as previously described [21]. Briefly, samples were centrifuged at 45,000 × *g* for 30 min at 4 °C and the supernatants precipitated using 20% TCA/acetone, w/v. Samples prepared for 2D SDS-PAGE were re-solubilised in buffer containing 8 M

urea, 2% CHAPS, w/v, 33 mM DTT, 0.5% carrier ampholytes (pH 3–10) (v/v) and protease inhibitors (CompleteMini, Roche, UK). A total of 300 μl containing 100 μg of ES product samples were used to actively rehydrate and focus 17 cm linear pH 3–10 IPG strips (Biorad, UK) at 20 °C for separation in the first dimension. All IPG strips were focussed between 60,000 and 65,000 Vh using the Protean IEF Cell (Biorad, UK). Each IPG strip was equilibrated for 15 min in 5 ml of equilibration buffer (containing 50 mM Tris–HCl pH 8.8, 6 M urea, 30% glycerol (v/v) and 2% SDS (w/v) [24]) with the addition of DTT (Melford, UK) at 10 mg/ml followed by a second equilibration with IAA (Sigma, UK) at 25 mg/ml replacing DTT. The IPG strips were separated in the second dimension on the Protean II system (Biorad, UK) using 12.5% polyacrylamide gels and run at 40 mA for approximately 1 h until through the stacking gel followed by 60 mA through the resolving gel until completion.

Gels were Coomassie blue stained (PhastGel Blue R, Amersham Biosciences, UK) and imaged with a GS-800 calibrated densitometer (Biorad, UK). Imaged 2-DE gels were analysed using Progenesis PG220 v.2006. Analysis was performed using mode of non-spot background subtraction on average gels created from a minimum of five biological replicates. Normalised spot volumes were calculated using the Progenesis 'total spot volume multiplied by total area' normalisation method. These normalised volumes were used to determine the degree of protein abundance change, up and/or down, between comparisons (with significance set at ±2-fold change). Significance of fold changes was confirmed by a one way ANOVA using LOG_{10} transformation, where appropriate, following a Kolmogorov–Smirnov test for normally distributed spot volumes. Unmatched protein spots were also detected between gel comparisons. Key protein spots of interest were excised and tryptically digested (modified trypsin sequencing grade, Roche, UK).

Protein spot data was taken from Progenesis and used for random forests (RF) analysis, an ensemble learning algorithm Breiman [25] as previously described [26]. RF analysis was performed using random-Forest (R software for random forest). Total protein secreted by each treatment was also recoded and was analysed by a two way ANOVA.

2.3. Spot excision and in-gel tryptic digestion

Protein spots were manually excised from SDS-PAGE and digested as previously described [23]. Briefly, excised protein spots were destained in 50% (v/v) acetonitrile (ACN) and 50 mM ammonium bicarbonate overnight at 4 °C until clear. Prior to digestion, protein spots were dehydrated in 100% ACN at 37 °C for 30 min. Gel plugs were rehydrated with 10 ng/μl trypsin in 50 mM ammonium bicarbonate for 45 min at 4 °C and allowed to incubate at 37 °C overnight. Post digestion 30 μl 60% (v/v) ammonium bicarbonate, 1% trifluroacetic acid was added to the gel plugs and sonicated in an ultra-sonicating water bath for 6 × 30 s bursts. Gel plugs were spun briefly at 16,000 × *g* and the supernatant removed and placed into a new tube. The addition of ammonium bicarbonate/trifluroacetic acid followed by sonication was repeated and the supernatants from both repeats were pooled. Supernatants were dried in a Maxi Dry Plus vacuum centrifuge (Hete-Holten A/S, Allerød, Denmark) and resuspended in 10 μl 1% (v/v) formic acid and sent for MSMS analysis.

2.4. Mass spectrometry and protein identification

Samples prepared for liquid chromatography–tandem mass spectrometry (LC–MS/MS) were analysed using electrospray ionisation as previously reported [27,28]. Peptide mixtures from trypsin digested gel spots were separated using a LC Packings Ultimate nano-HPLC System. Sample injection was *via* an LC Packings Famos auto-sampler and the loading solvent was 0.1% formic acid. The pre-column used was a LC Packings C18 PepMap 100, 5 mm, 100 A and the nano HPLC column was a LC Packings PepMap C18, 3 mm, 100 A. The solvent system was: solvent A (2% ACN with 0.1% formic acid), and solvent B (80% ACN with 0.1% formic acid). The LC flow rate was 0.2 μL/min with a gradient employed using 5% solvent A to 100% solvent B in 1 h. The HPLC eluent was sprayed into the nano-ES source of a Waters Q-TOFμMS *via* a New Objective Pico-Tip emitter. The MS was operated in positive ion mode and multiply charged ions were detected using a data-directed MS/MS experiment. Collision induced dissociation (CID) MS/MS mass spectra were recorded over the mass range *m/z* 80–1400 Da with scan time 1 s.

MassLynx v 3.5 (Waters, UK) ProteinLynx suite of tools was used to process raw fragmentation spectra. Each spectrum was combined and smoothed twice using the Savitzky–Golay method at ±3 channels with background noise subtracted at polynomial order 15 and 10% below curve. Monoisotopic peaks were centred at 80% centroid setting. Sequest compatible (.dta) file peak mass lists for each spectrum were exported, and spectra common to each 2DE spot were merged into a single MASCOT generic format (.mgf) file using the on-line Peak List Conversion Utility available at www.proteomecommons.org. Merged files were submitted to a MASCOT MS/MS ions search within a locally installed Mascot server (www.matrixscience.com) to search an 'in-house' database constructed from 6260 (858 763 residues) *F. hepatica* EST sequences downloaded and translated from the Sanger Institute (ftp://ftp.sanger.ac.uk/pub/pathogens/fasciola/hepatica/ESTs/).

Search parameters were as follows: enzyme set at trypsin with one missed cleavage allowed; fixed modifications were set for carbamidomethylation with variable modifications considered for set as the oxidation of methionine; monoisotopic masses with unrestricted protein masses were considered with peptide and fragment mass tolerances at ±1.2 Da and ±0.6 Da respectively for an ESI-QUAD-TOF instrument. Protein identifications resulting from MASCOT ions scores greater than 25 were considered as showing significant identity or extensive similarity ($p < 0.05$) to the predicted identification displayed (www.matrixscience.com).

Spectra that did not match any proteins, or scored non-significantly within *F. hepatica* EST database were re-searched through MASCOT against the NCBI non-redundant database (NCBI http://www.ncbi.nlm.nih.gov/nr release 20091112 containing 10,032,801 sequences; 3,422,028,181 residues). MASCOT scores for individual ions greater than 23 indicated significant similarity whilst scores above 51 indicate significant identity or extensive similarity ($p < 0.05$). All MASCOT

search parameters and settings were as described above except that taxonomy was restricted to 'Metazoa' (1804634 sequences).

F. hepatica proteins identified *via* LC–MS/MS matching unannotated ESTs, were assigned putative identification based upon similarity to proteins with existing annotation within GenBank non-redundant database (all non-redundant GenBank CDS translations + PDB + SwissProt + PIR + PRF excluding environmental samples from WGS projects (9,636,254 sequences; 3,294,494,089 total letters: Posted date: Sep 2, 2009 5:42 PM; Downloaded at ftp://ftp.ncbi.nih.gov/blast/db/).

3. Results

3.1. Survival

The viability of liver fluke *in vitro* maintenance was assessed at each change of media and was based on standard visible motility of worms and worm shape [27]. All control samples (Con) with the exception of one replicate showed 100% viability after 26 h *in vitro* maintenance (Fig. 1a). The remaining control replicate showed no motility in any of the 10 fluke post 26 h although all were alive post 14 h. All sub-lethal (SL) samples showed 100% viability (Fig. 1A), although showed an altered 'curled and extended' phenotype post maintenance. Post 26 h *in vitro* maintenance all lethal (L) samples presented with no motility and recorded as dead [27] (Fig. 1A). Survival for all 'lethal' replicates declined rapidly post 8 h in maintenance culture.

3.2. ES product protein content

Collected samples were assessed for their ES protein content to identify trends as a response to TCBZ-SO treatment. Initial protein release post 2 h incubation showed no significant differences between Con and SL and L treated samples (Fig. 1B). Both treatment (TCBZ-SO Con, SL & L doses) ($P_{2,71} = 0.043$) and time ($P_{3,71} \leq 0.001$) had a significant effect on the level of protein expressed. There was a significant treatment × time interaction ($P_{6,71} = 0.005$) thereby demonstrating that the effect of time on the level of protein expressed was dependent on the treatment administered. In general, protein release decreased over time *in vitro* maintenance. Notable differences were seen post 14 and 26 h. At 14 h in maintenance culture, protein secretion had dropped significantly with control samples secreting the most; Con > SL > L. Post 26 h, a large increase in released protein was seen in the lethal samples only.

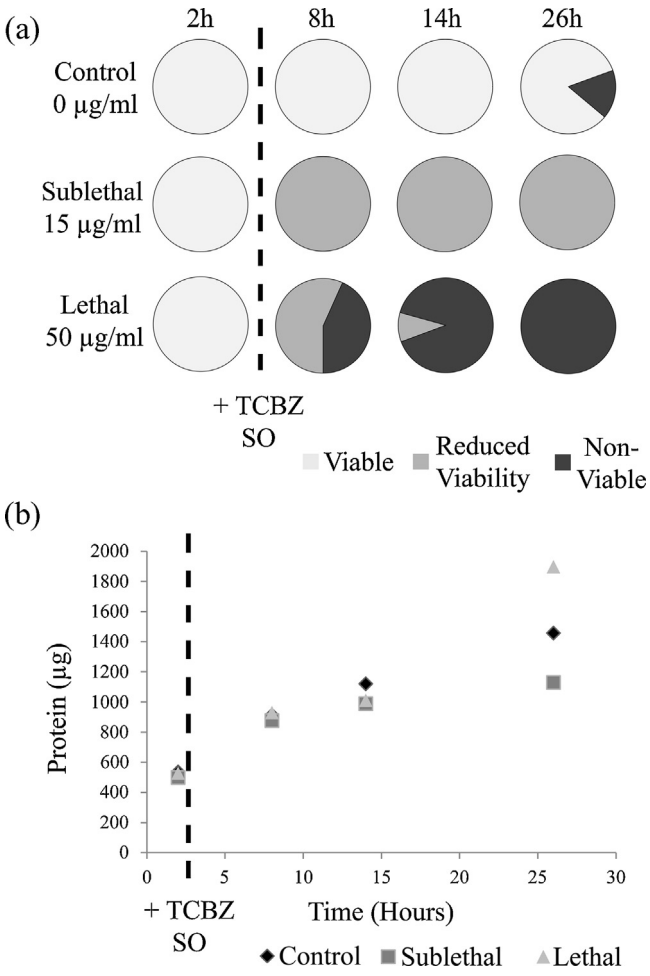

Fig. 1 – *F. hepatica* survival and protein secretion under TCBZ-SO stress (control 0 µg/ml, sub-lethal 15 µg/ml and lethal 40 µg/ml) (a) graphical view of *F. hepatica* survival (expressed as %) *in vitro* maintenance under each TCBZ-SO dose regime over the course of the experiment in hours (h). Viable – fluke expressing normal motility and appearance; reduced viability – motility reduced, muscle tension and morphological changes; non-viable – apparent death, no motility and flaccid musculature. (b) Cumulative protein content (µg) secreted/excreted from liver fluke *in vitro* maintenance under control, sub-lethal or lethal TCBZ-SO conditions over time (h). Dashed lines in both (a) and (b) indicate the addition of TCBZ-SO at the appropriate concentration after 2 h *in vitro* culture.

3.3. ES product proteomic arrays

Proteomic 2D arrays produced reproducible replicates among treatments. Matching between treatment replicates was between 50 and 75% with the average matching at 58.3% (Supplementary Table 1). Only one set of replicates, sub-lethal 14–26 h, failed to match within these limits and had a low match percentage of 35%. This low percentage matching relates to the low level of protein secreted by these worms, often lower than 50 µg in total (Fig. 1B). All replicate matches and total spot numbers can be seen in Supplementary Table 2.

After 2 h *in vitro* maintenance there was, as expected, low variation between treatments (all liver fluke in control conditions from 0 to 2 h; Supplementary Fig. 1). Thus, a high percentage of replicate matching at this stage provided the confidence needed to assess two sets of replicates with TCBZ SO at SL and L doses.

After 8 h only 1 protein spot (spot 13, Fig. 2 SL and L 2–8 h) showed a significant change in abundance, a significant reduction with increasing TCBZ-SO concentrations (spot 13 $F_{2,15} = 11.14$, $P = 0.001^{***}$) to complete absence in Lethal samples. In addition, a further protein spot was unique to SL and

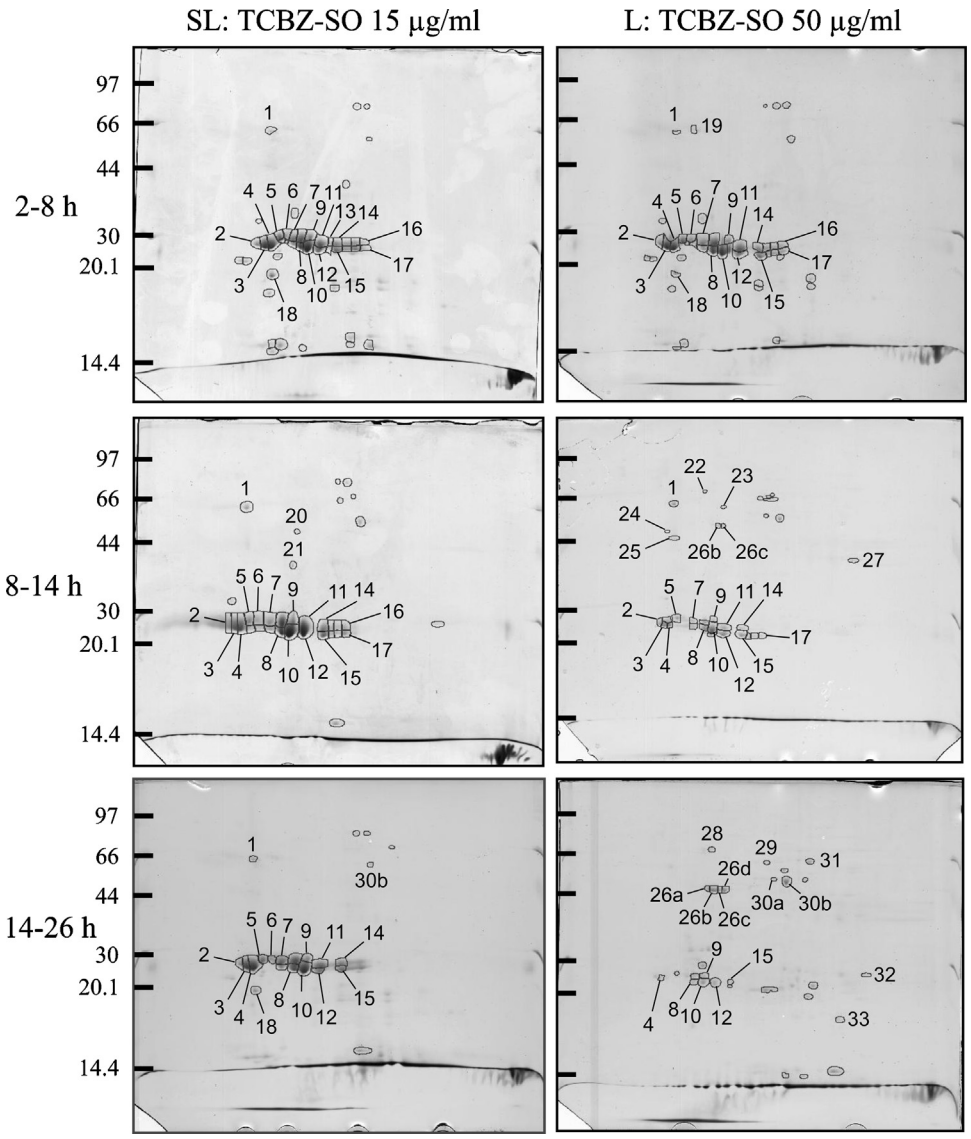

Fig. 2 – Representative 2DE SDS-PAGE arrays of *F. hepatica* ES products under TCBZ-SO stress at sub-lethal (SL) and lethal (L) concentrations (15 and 50 µg/ml, respectively) over three time periods, 2–8 h, 8–14 h and 14–26 h. TCBZ-SO induced ES products were profiled on 12.5% polyacrylamide gels and stained with coomassie blue. Proteins were isoelectric focused on 17 cm pH 3–10 linear immobilised pH gradient (IPG) strips. Circled spots correspond to those proteins consistently present on averaged gels for each treatment. Numbered protein spots, in conjunction with Table 1, correspond to abundance changes compared to control ES products at the corresponding time point and their putative protein identifications can be found in Table 1.

L treatments (spot 1, Fig. 2). Lethal samples also showed an additional unique spot (Fig. 2, spot 19).

Post 14 h *in vitro* maintenance the majority of changes resulting from *in vitro* treatment with TCBZ-SO were seen. A total of 22 protein spots (Fig. 2 SL and L 8–14 h spots 1, 4–11, 13–14, 16–17 and 20–27 [excluding 26A and D]) showed significant variation between treatments. Of the 22 significant spots, 11 normalised spot volumes were consistent between Con and SL samples. The significant variation observed was when comparing L samples to Con and SL, showing significant reductions in these protein spots (spots 4–11, 14 and 16–17; see Supplementary Table 3 for spot differential abundance statistics). The remaining 11 significant spots, with the exception of spot 13, were additional/unique protein spots when compared to Con samples; spots 1, 20 and 21 for SL and 1 and 22–27 (excluding 26 A and D) for L samples. The final spot of significant change was that of spot 13 reduced in abundance to absence in both SL and L samples.

Samples *in vitro* maintenance post 26 h showed significant variation relating to levels of TCBZ-SO. A total of 27 protein spots (Fig. 2 and Table 1) varied in abundance with 17 of these (spots 2–15, 18 and 30A and B) changing with increasing levels of TCBZ-SO in both SL and L samples. The remaining 10 spots (Fig. 2, spots 1, 26A–D, 28–29 and 31–33) were additional/unique protein spots when compared to Con samples with all, with

Table 1 – Putative protein identifications of *F. hepatica* TCBZ-SO induced ES products using MASCOT. Spectra from mass spectrometry were subjected to MSMS ion searches using MASCOT (Matrix Science) searching an in house EST database. Significant hits, at P = 5%, have a MASCOT score of 25 or greater. All significant EST hits were then subjected to BLAST analysis against GenBank to assign an identity to matching ESTs. Therefore, all reported accession numbers are from GenBank.

Spot number	MS/MS ion search			Highest scoring BLAST hit within GenBank				Protein Variation[a]		
	F. hepatica EST hit	MASCOT score	Peptides matched	Protein	Organism	Accession number	E-value	2–8 h	8–14 h	14–26 h
1	NS	–	–	–	–	–	–	SL, L	SL, L	SL
2	Fhep43c03.q1k	53	2	Secreted cathepsin L2 (CL2)	*F. hepatica*	ABQ95351	1.00E−108			L−[b]
	Fhep06c12.q1k	52	1	Cathepsin L (CL5)	*F. hepatica*	AAF76330	1.00E-112			
	Fhep44h05.q1k	52	1	Cathepsin L (CL5)	*F. hepatica*	AAF76330	1.00E−116			
	Fhep55g09.q1k	52	1	Cathepsin L (CL5)	*F. hepatica*	AAF76330	1.00E−135			
3	Fhep43c03.q1k	356	14	Secreted cathepsin L2 (CL2)	*F. hepatica*	ABQ95351	3.94E−106			SL− L−[b]
	Fhep54d04.q1k	356	14	Secreted cathepsin L2 (CL2)	*F. hepatica*	ABQ95351	4.07E−110			
	Fhep42b08.q1k	207	9	Secreted cathepsin L2 (CL2)	*F. hepatica*	ABQ95351	1.00E−127			
	Fhep48f01.q1k	207	9	Secreted cathepsin L2 (CL2)	*F. hepatica*	ABQ95351	1.00E−114			
	Fhep48f09.q1k	191	6	Cathepsin L-Like Protease (CL2)	*F. hepatica*	CAA80446	1.00E−119			
	Fhep38a03.q1k	191	7	Secreted cathepsin L2 (CL2)	*F. hepatica*	ABQ95351	1.00E−146			
4	Fhep43c03.q1k	345	15	Secreted cathepsin L2 (CL2)	*F. hepatica*	ABQ95351	3.94E−106		L−	SL− L− −
	Fhep35b02.q1k	214	9	Cathepsin L1D (CL1D)	*F. hepatica*	ACJ12893/4	1.00E−70			
	Fhep35d02.q1k	214	9	Cathepsin L1D (CL1D)	*F. hepatica*	ACJ12894	3.00E−83			
	Fhep47f09.q1k	214	9	Cathepsin L1D (CL1D)	*F. hepatica*	ACJ12893/4	1.00E−66			
	Fhep42b08.q1k	152	9	Secreted cathepsin L2 (CL2)	*F. hepatica*	ABQ95351	1.00E−127			
5	Fhep07e08.q1k	173	9	Cathepsin L (CL5)	*F. hepatica*	AAF76330	1.00E−119		L−	L−
	Fhep39a05.q1k	103	8	Cathepsin L (CL5)	*F. hepatica*	AAF76330	1.00E−138			
	Fhep47g05.q1k	34	1	Cathepsin L (CL5)	*F. gigantica*	ABV90500	9.00E−39			
	HAN5016f11.q1kT3	34	1	Cathepsin L (CL5)	*F. gigantica*	ABV90500	1.00E−64			
	Fhep40g12.q1k	32	3	NS	–	–	–			
6	Fhep07e08.q1k	144	7	Cathepsin L (CL5)	*F. hepatica*	AAF76330	1.00E−119		L−[b]	L−[b]
	Fhep37h07.q1k	144	7	Cathepsin L (CL5)	*F. hepatica*	AAF76330	1.00E−120			
	HAN5020e07.p1kT7	67	4	Cathepsin L (CL1A)	*F. hepatica*	AAM11647	1.00E−138			

7	Fhep07e08.q1k	153	5	Cathepsin L (CL5)	*F. hepatica*	AAF76330	1.00E−119		L−	L−
	Fhep37h07.q1k	153	5	Cathepsin L (CL5)	*F. hepatica*	AAF76330	1.00E−120			
	Fhep10h09.q1k	153	5	Cathepsin L (CL5)	*F. hepatica*	AAF76330	1.00E−110			
	Fhep44a04.q1k	101	6	Cathepsin L (CL1D)	*F. gigantica*	ABV90502	9.00E−77			
8	Fhep20f07.q1k	258	9	Secreted cathepsin L1 (CL1A)	*F. hepatica*	AAB41670	6.00E−84		SL+ L−	L−
	Fhep47e11.q1k	258	9	Cathepsin L protein (CL1A)	*F. hepatica*	AAR99518	2.00E−95			
	Fhep54a06.q1k	258	9	Secreted cathepsin L1 (CL1A)	*F. hepatica*	AAB41670	8.00E−84			
	Fhep45a09.q1k	240	10	Cathepsin L-like proteinase (CL1A)	*F. hepatica*	Q24940	5.00E−93			
	Fhep44h04.q1k	205	10	Cathepsin L protein (CL1A/B)	*F. hepatica*	AAR99519	1.00E−112			
9	Fhep11e04.q1k	93	4	Cathepsin L1D (CL1D)	*F. hepatica*	ACJ12894	2.00E−85		L−	SL− L−
	Fhep21a11.q1k	93	4	Cathepsin L1D (CL1D)	*F. hepatica*	ACJ12894	1.00E−106			
	Fhep41d11.q1k	93	4	Cathepsin L1D (CL1D)	*F. hepatica*	ACJ12894	1.00E−99			
10	Fhep21a11.q1k	288	12	Cathepsin L1D (CL1D)	*F. hepatica*	ACJ12894	1.00E−106		L−	SL− L− −
	Fhep41d11.q1k	288	12	Cathepsin L1D (CL1D)	*F. hepatica*	ACJ12894	1.00E−99			
11	Fhep45a09.q1k	149	9	Cathepsin L-like proteinase (CL1A)	*F. hepatica*	Q24940	5E−93		L−	SL− L− −[b]
12	Fhep20f07.q1k	373	14	Secreted cathepsin L1 (CL1A)	*F. hepatica*	AAB41670	6.00E−84			SL− L−
13	Fhep20f07.q1k	401	12	Secreted cathepsin L1 (CL1A)	*F. hepatica*	AAB41670	6.00E−84	SL− L−[b]	SL−[b] L−[b]	SL−[b] L−[b]
	Fhep47e11.q1k	401	12	Cathepsin L protein (CL1A)	*F. hepatica*	AAR99518	2.00E−95			
	Fhep54a06.q1k	401	12	Secreted cathepsin L1 (CL1A)	*F. hepatica*	AAB41670	8.00E−84			
14	Fhep20f07.q1k	137	5	Secreted cathepsin L1 (CL1A)	*F. hepatica*	AAB41670	6.00E−84		L−	L−[b]
	Fhep47e11.q1k	137	5	Cathepsin L protein (CL1A)	*F. hepatica*	AAR99518	2.00E−95			
	Fhep54a06.q1k	137	5	Secreted cathepsin L1 (CL1A)	*F. hepatica*	AAB41670	8.00E−84			
15	Fhep11e04.q1k	135	6	Cathepsin L1D (CL1D)	*F. hepatica*	ACJ12894	2.00E−85			SL− L−
	Fhep21a11.q1k	135	6	Cathepsin L1D (CL1D)	*F. hepatica*	ACJ12894	1.00E−106			
	Fhep41d11.q1k	135	6	Cathepsin L1D (CL1D)	*F. hepatica*	ACJ12894	1.00E−99			

Table 1 – (*Continued*)

Spot number	MS/MS ion search			Highest scoring BLAST hit within GenBank				Protein Variation[a]		
	F. hepatica EST hit	MASCOT score	Peptides matched	Protein	Organism	Accession number	*E*-value	2–8 h	8–14 h	14–26 h
16	Fhep07d09.q1k	235	7	Cathepsin L-like proteinase (CL1A)	*F. hepatica*	Q24940	1.00E−105		L−[b]	
	Fhep45a09.q1k	235	7	Cathepsin L-like proteinase (CL1A)	*F. hepatica*	Q24940	5.00E−93			
	Fhep47g04.q1k	235	7	Cathepsin L-like proteinase (CL1A)	*F. hepatica*	Q24940	5.00E−83			
	Fhep20f07.q1k	205	7	Secreted cathepsin L1 (CL1A)	*F. hepatica*	AAB41670	6.00E−84			
	Fhep47e11.q1k	205	7	Cathepsin L protein (CL1A)	*F. hepatica*	AAR99518	2.00E−95			
	Fhep43c04.q1k	205	7	Secreted cathepsin L1 (CL1A)	*F. hepatica*	AAB41670	2.00E−83			
17	Fhep20f07.q1k	145	7	Secreted cathepsin L1 (CL1A)	*F. hepatica*	AAB41670	6.00E−84		L−	
	Fhep47e11.q1k	145	7	Cathepsin L protein (CL1A)	*F. hepatica*	AAR99518	2.00E−95			
	Fhep54a06.q1k	145	7	Secreted cathepsin L1 (CL1A)	*F. hepatica*	AAB41670	8.00E−84			
	Fhep36f11.q1k	60	2	Thioredoxin Peroxidase	*F. gigantica*	ABY85785	1.00E−107			
18	Fhep05a08.q1k	54	1	Secreted cathepsin L2 (CL2)	*F. hepatica*	ABQ95351	6.00E−64			SL+ L−[b]
	Fhep46a02.q1k	54	1	Secreted cathepsin L2 (CL2)	*F. hepatica*	ABQ95351	1.00E−101			
	Fhep35d02.q1k	54	1	Cathepsin L1D (CL1D)	*F. hepatica*	ACJ12894	3.00E−83			
	Fhep43c03.q1k	50	2	Secreted cathepsin L2 (CL2)	*F. hepatica*	ABQ95351	3.94E−106			
	Fhep54d04.q1k	50	2	Secreted cathepsin L2 (CL2)	*F. hepatica*	ABQ95351	4.07E−110			
19	NS	–	–	–	–	–	–	L		
20	Fhep10b05.q1k	78	2	Cathepsin L1D (CL1D)	*F. hepatica*	ACJ12894	4.00E−70		SL	
	Fhep21a11.q1k	78	2	Cathepsin L1D (CL1D)	*F. hepatica*	ACJ12894	1.00E−106			
	Fhep46e07.q1k	78	2	Cathepsin L1D (CL1D)	*F. hepatica*	ACJ12894	2.00E−99			
	Fhep50d05.q1k	30	3	Protein Disulphide Isomerase	*F. hepatica*	CAA12644	1.00E−151			
	Fhep37e03.q1k	28	2	SJCHGC06296 Protein	*S. japonicum*	AAW25214	2.00E−27			
	Fhep37e03.q1k	28	2	Similar to NM_003344 Ubiquitin-Conjugating Enzyme E2H in Mus musculus	*S. mansoni*	AAP06436	3.00E−27			
	Fhep22a12.q1k	27	1	Coatomer Gamma Subunit	*S.mansoni*	XP_002580249	2.00E−96			

21	Fhep05c11.q1k	97	1	Cathepsin L1D (CL1D)	*F. hepatica*	ACJ12893	4.00E−46	SL	
	Fhep13h03.q1k	97	1	Cathepsin L-like proteinase (CL1A)	*F. hepatica*	Q24940	1.00E−84		
	Fhep25g09.q1k	97	1	Cathepsin L-like proteinase (CL1A)	*F. hepatica*	Q24940	1.00E−124		
22	NS	–	–	–	–	–	–	L	
23	NS	–	–	–	–	–	–	L	
24	NS	–	–	–	–	–	–	L	
25	NS	–	–	–	–	–	–	L	
26A	Fhep45a09.q1k	106	2	Cathepsin L-like proteinase (CL1A)	*F. hepatica*	Q24940	5.00E−93		L
	Fhep40g02.q1k	103	2	Cathepsin L-Like (CL1B)	*F. hepatica*	AAK38169	1.00E−23		
	HAN4008f12.q1kT3	95	6	Gelsolin	*S. mansoni*	XP_002572344	2.00E−74		
26B	HAN4008f12.q1kT3	128	6	Gelsolin	*S. mansoni*	XP_002572344	2.00E−74	L	L
	Fhep09a08.q1k	124	6	Actin	*S. mansoni*	XP_002575979	1.00E−111		
	Fhep22a04.q1k	90	6	Actin	*S. mansoni*	XP_002578518	1.00E−104		
	Fhep34c01.q1k	87	3	Actin	*Stictodora lari*	AAS20346	4.00E−79		
	HAN3008-1g11.q1k	72	4	Actin	*S. mansoni*	XP_002578518	1.00E−123		
26C	Fhep09a08.q1k	151	6	Actin	*S. mansoni*	XP_002575979	1.00E−111	L	L
	HAN3008-1g11.q1k	44	6	Actin	*S. mansoni*	XP_002578518	1.00E−123		
	Fhep22a04.q1k	44	3	Actin	*S. mansoni*	XP_002578518	1.00E−104		
	HAN4003e07.p1kT7	32	1	Actin	*S. mansoni*	XP_002578518	1.00E−40		
	HAN4003e07.q1kT3	32	1	SJCHGC06318 Protein	*S. japonicum*	AAW25537	1.00E−75		
	HAN4008a06.p1kT7	32	1	SJCHGC06318 Protein	*S. japonicum*	AAW25537	6.00E−70		
	HAN4008a06.p1kT3	32	1	Actin	*S. mansoni*	XP_002578518	5.00E−71		
	HAN5015g10.q1kT3	32	1	SJCHGC06318 Protein	*S. japonicum*	AAW25537	3.00E−62		
26D	Fhep34c01.q1k	98	2	Actin	*Stictodora lari*	AAS20346	4.00E−79		L
	Fhep09a08.q1k	97	4	Actin	*S. mansoni*	XP_002575979	1.00E−111		
	HAN4003e07.p1kT7	58	2	Actin	*S. mansoni*	XP_002578518	1.00E−40		
	HAN4003e07.q1kT3	58	2	SJCHGC06318 Protein	*S. japonicum*	AAW25537	1.00E−75		
	HAN4008a06.p1kT7	58	2	SJCHGC06318 Protein	*S. japonicum*	AAW25537	6.00E−70		
	HAN4008a06.p1kT3	58	2	Actin	*S. mansoni*	XP_002578518	5.00E−71		
	HAN5015g10.q1kT3	58	2	SJCHGC06318 Protein	*S. japonicum*	AAW25537	3.00E−62		
	HAN3008-1g11.q1k	51	6	Actin	*S. mansoni*	XP_002578518	1.00E−123		
27	Fhep15d10.q1k	60	2	Glyceraldehyde-3-phosphate dehydrogenase	*F. hepatica*	AAG23287	2.00E−82	L	
28	Fhep07e08.q1k	131	4	Cathepsin L (CL5)	*F. hepatica*	AAF76330	1.00E−119		L
	Fhep10h09.q1k	131	4	Cathepsin L (CL5)	*F. hepatica*	AAF76330	1.00E−110		

Table 1 – (*Continued*)

Spot number	MS/MS ion search			Highest scoring BLAST hit within GenBank				Protein Variation[a]		
	F. hepatica EST hit	MASCOT score	Peptides matched	Protein	Organism	Accession number	E-value	2–8 h	8–14 h	14–26 h
29	Fhep07d09.q1k	120	2	Cathepsin L-like proteinase (CL1A)	*F. hepatica*	Q24940	1.00E−105			L
	Fhep45a09.q1k	120	2	Cathepsin L-like proteinase (CL1A)	*F. hepatica*	Q24940	5.00E−93			
	Fhep47g04.q1k	120	2	Cathepsin L-like proteinase (CL1A)	*F. hepatica*	Q24940	5.00E−83			
30A	Fhep28b10.q1k	147	7	Enolase	*F. hepatica*	AAA57450	1.00E−91			L+
30B	Fhep28b10.q1k	147	7	Enolase	*F. hepatica*	AAA57450	1.00E−91			SL+, L++
31	NS	–	–	–	–	–	–			L
32	Fhep26g11.q1k	137	4	Multivalent Antigen sjTPI-97	Synthetic Construct	ABS19444	7.00E−89			L
	Fhep26g11.q1k	137	4	Triose-Phosphate Isomerase	*Orientobilharzia turkestanicum*	AAZ57433	6.00E−87			
33	Fhep05f07.q1k	97	4	SJCHGC05973 Protein (DJ-1)	*S. japonicum*	AAW26651	3.00E−54			L
	HAN4008f12.p1kT7	74	2	SJCHGC06031 Protein	*S. japonicum*	AAX25657	3.00E−66			
	HAN4008f12.q1kT3	74	2	Gelsolin	*S. mansoni*	XP_002572344	2.00E−74			
	Fhep29e10.q1k	37	3	GJ21252 (Cyclophilin)	*Drosophila virilis*	XP_002048823	4.00E−56			

[a] When compared to control ES products, at the corresponding time point, protein spots showing a change in abundance are denoted. If a unique protein spot is found in the sub-lethal (TCBZ-SO at 15 μg/ml) ES products they are denoted with SL. If a unique protein spot is found in the lethal (TCBZ-SO at 50 μg/ml) ES products they are denoted with L. If followed by + − they are not unique compared to controls but are more than 2-fold up/down regulated.

[b] Denotes an absence of the protein spot from the array compared to control (TCBZ-SO at 0 μg/ml) ES products. Those indications shaded in grey were identified as 2-fold up/down regulated but not statistically significant, see also Supplementary Table 3 for all statistics. Full peptide identifications following MSMS can be found in Supplementary Table 4.

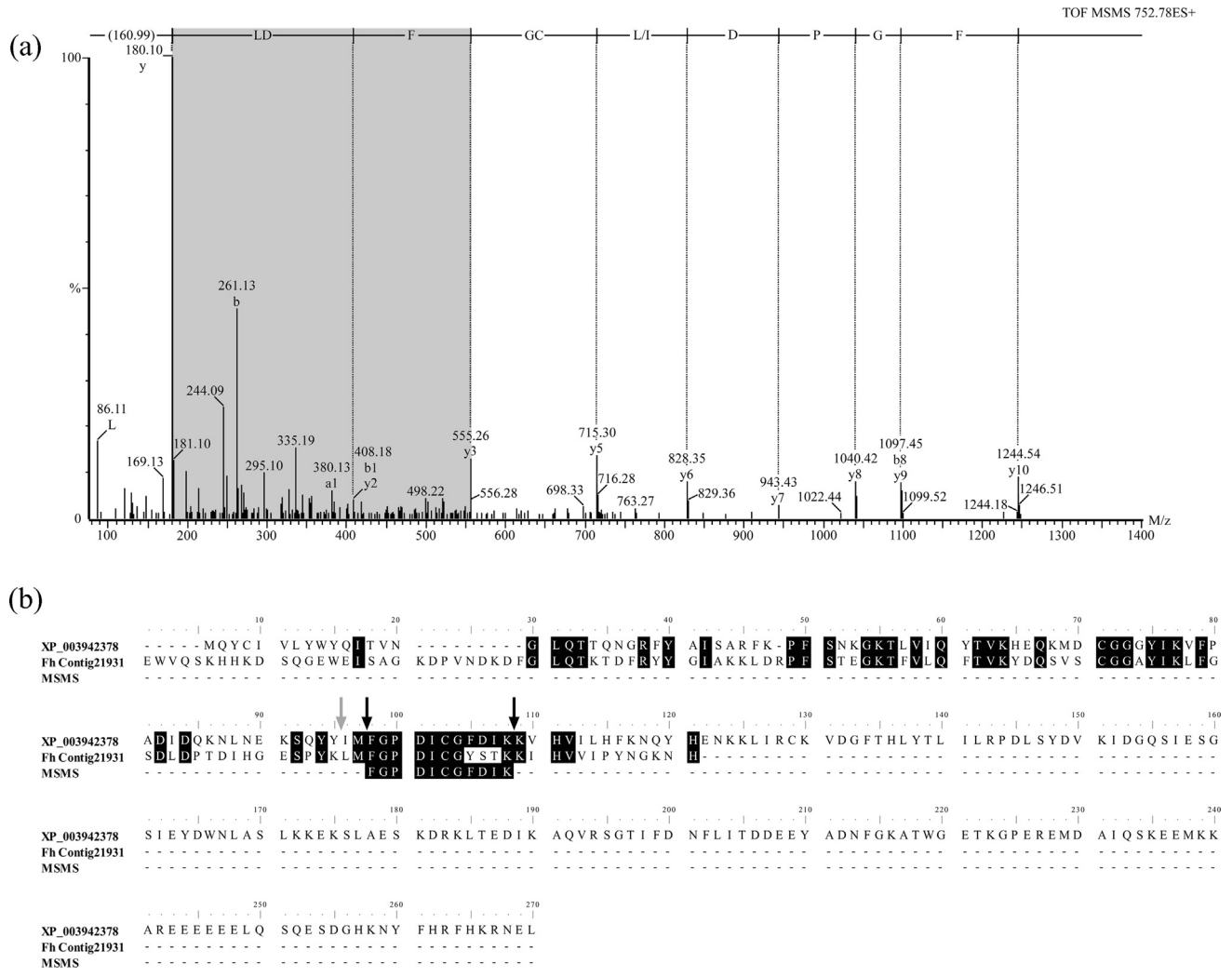

Fig. 3 – Evidence for the putative identification of calreticulin. (a) MSMS spectra from the analysis of a 2^+ peptide *m/z* 752.78 (sequence FGPDICGFDIK) sequenced from protein spot 1 (Fig. 2 and Table 1), identified as calreticulin-3 of *Saimiri boliviensis*. Predicted residues shaded in grey highlight amino acids that do not match with a *F. hepatica* Contig. Sequencing was performed automated using MassLynx v 3.5. (b) Multiple alignment of calreticulin from *S. boliviensis* (XP_003942378), the matching *F. hepatica* transcript (Fh Contig21931) and the sequence derived from tandem mass spectrometry (MSMS). Amino acid residues boxed in black represent 100% matching among sequences. Black arrows indicate the start and end of the sequence tag identified from tandem mass spectrometry. The grey arrow indicates the start of the matching theoretical tryptic peptide.

the exception of spot 1, unique to L samples. All spot variations can be seen in Table 1.

3.4. *Protein identification*

All 33 protein spots of interest highlighted by 2D arrays were analysed by MSMS (Table 1). Of these 33, only 7 could not be identified using MSMS ion scans with an in-house EST database and matching ESTs to a Genbank entry. The greatest number of identifications was *F. hepatica* cathepsin L proteases with 22 protein spots. The majority of these identifications were from spots reduced in abundance, and ultimate absence, of Cathepsin L proteases in L samples after 14 and 26 h *in vitro* maintenance.

Of particular interest were spots 26A–D, identified as actin and gelsolin, appearing in ES samples after 14 and 26 h *in vitro* maintenance at L levels only and spots 30A and B, identified as enolase, increasing in abundance after 26 h in both SL and L *in vitro* maintenance cultures. Also identified only in L *in vitro* maintenance after 26 h were triose phosphate isomerase and DJ-1 (Fig. 2 and Table 1 spots 32 and 33, respectively).

Of the seven protein spots unidentified by MSMS ion scans spot 1 appeared to be of significant interest. Spot 7 was identified in response to TCBZ-SO exposure after 8, 14 and 26 h *in vitro* maintenance in SL samples and after 8 and 14 h in L samples. In order to identify this protein MSMS spectra from replicate samples were *de novo* sequenced. This repeatedly identified a 2^+ peptide of *m/z* 752.78 and sequenced

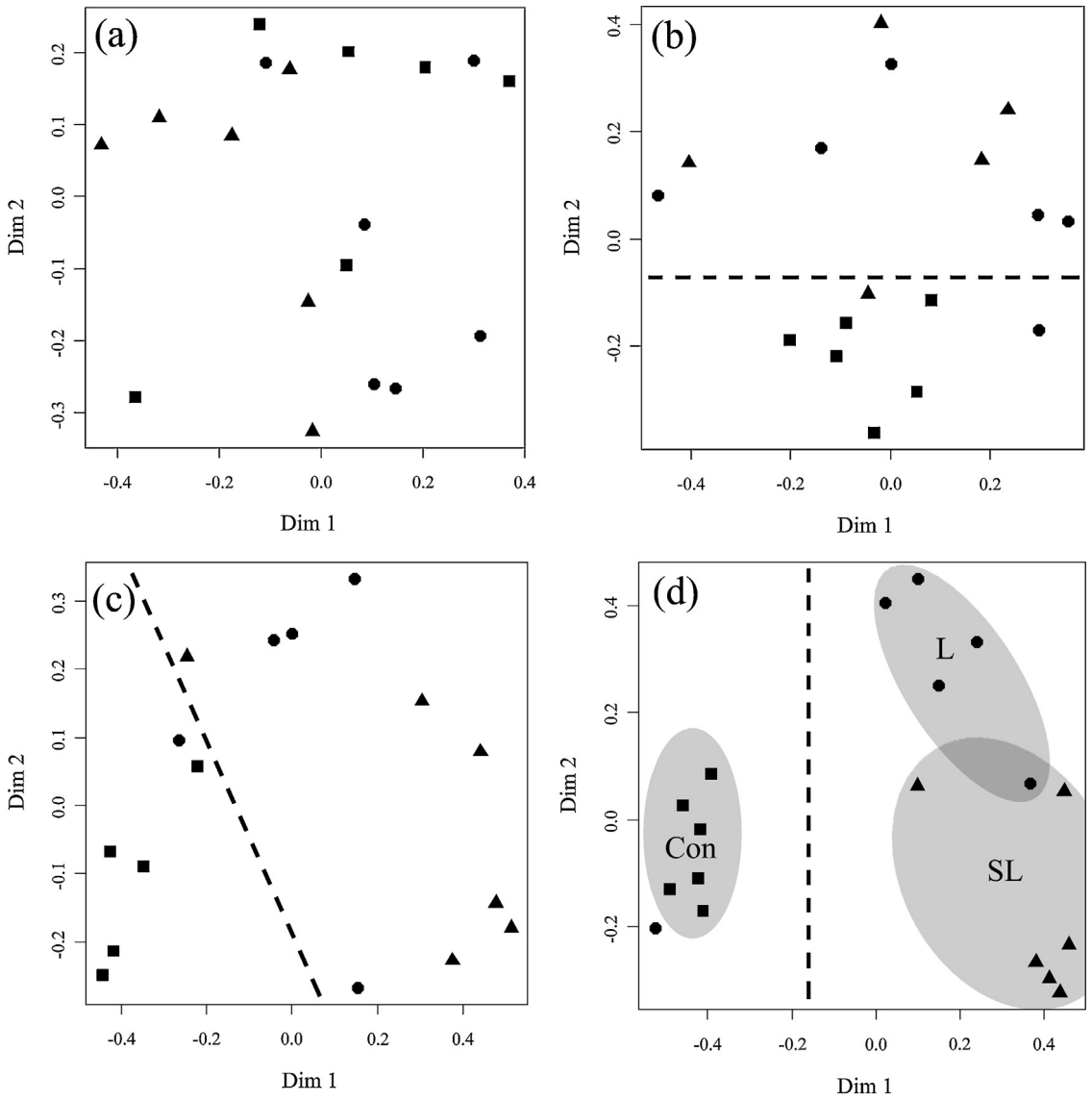

Fig. 4 – Dimension plots from random forest analysis of ES product proteomes using normalised spot volumes for control (Con: black closed squares), sub-lethal (SL: black closed triangles) and lethal (L: black closed circles) TCBZ-SO regimes. Dimension plots are from ES products after 2 h (a), 8 h (b), 14 h (c) and 26 h (d). Dashed lines represent separation between drug exposed and control samples. Separation between control samples and TCBZ-SO exposed samples occurs after 8 h with almost complete separation of treatment groups after 26 h *in vitro* maintenance.

as FGPDICGFDIK (Fig. 3A). When using BLAST to assign a putative identification to this peptide calreticulin-3 (Genbank: XP_003942378 Organism: *Saimiri boliviensis* Coverage: 100% E value: 0.004) was hit. The resulting sequence was used to search a *F. hepatica* transcriptome database (EBI-ENA archive ERP000012: an initial characterisation of the *F. hepatica* transcriptome using 454-FLX sequencing) for a *Fasciola* specific sequence. When a matching contig (Contig21931) was compared to the *de novo* sequenced peptide, three amino acid residues were not consistent between the two sequences (Fig. 3B) despite good sequence similarity between the *F. hepatica* sequence and the *S. boliviensis* sequence over this small region (Amino acid residues 83–93; XP_003942378 numbering). However, the quality of the MSMS generated mass spectrum spanning these three amino acid residues (Fig. 3A shaded in grey) was repeatedly low making *de novo* interpretation of these three residues challenging.

3.5. *Random forests (RF) analysis*

After subjecting *F. hepatica* to TCBZ-SO exposure *in vitro* maintenance, RF analysis was performed to assess the impact of the 2D protein arrays and the ability to distinguish between TCBZ-SO treatment proteomes; namely Con, SL or L TCBZ-SO regimes. Post 2 h *in vitro* maintenance, no distinct separation of treatment groups could be identified corresponding to a low clustering coefficient (clustering coefficient 0–2 h = 0.44) seen in the resulting dimension plots (Fig. 4A). This was despite of increasing RF tree numbers to 100,000 thereby encompassing all variables (protein spots).

As early as 8 h in maintenance a distinction between Con and TCBZ-SO exposed samples (SL and L) is almost apparent (Fig. 4B). However, there was no separation between SL and L samples again related to a low clustering coefficient (2–8 h = 0.48). At 8–14 h samples begin to discriminate into three clusters associated with treatment, Con, SL and L doses (clustering coefficient 8–14 h = 0.53) still with a defined separation between Con and TCBZ-SO exposed samples (Fig. 4C). After 14–26 h *in vitro* maintenance, clear separation between groups can be identified again based on treatment (Fig. 4D: clustering coefficient 14–26 h = 0.67).

4. Discussion

We have shown measurable differences in the released protein signature of adult *F. hepatica* when TCBZ-SO exposed and killed, suggesting that potential biomarkers are released into the host environment to determine TCBZ resistance and susceptibility. In addition, we have identified a protein signature released by *F. hepatica* during *in vitro* exposure to a sub-lethal dose of drug, a potentially new approach to measure drug failure in the field as a consequence of sub-optimal or incorrect dosing.

We have also identified the multifunctional Ca^{2+} binding protein calreticulin (CRT) as a new biomarker of TCBZ-SO exposure and survival as judged by post-proteomic image analysis and RF analysis *i.e.* only liver fluke exposed to TCBZ-SO, at both studied concentrations (SL and L), that were alive released CRT into ES products. Those that had died at a lethal dose of TCBZ-SO after 26 h ceased to release CRT into the ES products. CRT from parasitic helminths has a variety of suggested functions [29–31]. However, perhaps more significant is the finding of CRT in the interaction of other helminths and anthelmintic compounds.

Mutapi et al. [32] studying the related *S. haematobium* observed that CRT was recognised by human sera following infection and subsequent treatment with praziquantel (PZQ). Therefore, does CRT have a similar role in both TCBZ-SO and PZQ exposure and/or is it a novel generic biomarker of flatworm drug response. It has been shown in parasitic species that increases in CRT levels can be activated by a variety of biological or, more pressing, chemical stressors [33]. It is likely that the recognised protein chaperoning function of CRT (Gene Ontology terms – GO: 0006457 Protein folding and GO: 0051082 unfolded protein binding), preventing aggregation of unfolded proteins [34], is the primary reason for an increase following stress. However, regarding anthelmintic stress, it is suspected that PZQ increases membrane permeability to cations, such as Ca^{2+} [35]. As a result, an increase in CRT expression may be an attempt to reduce store operated Ca^{2+} influx [36] in order to balance Ca^{2+} homeostasis [34,37]. It is therefore possible that TCBZ-SO exposure in *Fasciola* may also affect Ca^{2+} homeostasis.

Alternatively, in the current study, increased CRT released into ES products may also result from xenobiotic induced necrosis from incorrect Ca^{2+} homeostasis – show in *C. elegans* for stressors not affecting Ca^{2+} influx across the plasma membrane [38].

Aside from CRT, the cathepsin L (Cat L) proteases were also revealed as significant in determining TCBZ-SO exposure and correct drug dosing and drug failure. The Cat L proteases contribute significantly to the ES products of *F. hepatica* [21,39], with family members continually secreted and regurgitated into the host environment. Therefore, a change in abundance of this important family of virulence proteins, in relation to TCBZ-SO exposure, would be expected. Indeed, a reduction in the viability of flukes exposed to TCBZ-SO was observed with a concomitant decrease in Cat L protease release; results comparable with studies on levamisole treated *H. contortus* revealing a 50% reduction of Cat L proteases post treatment [40].

The glycolytic enzyme enolase can be readily found in ES products of *F. hepatica* [21,41] or associated with membrane fractions [42,43], but here we have identified enolase as an ES product determinant of TCBZ-SO exposure; up-regulated in ES products after 26 h in both SL and L treatments. We have also previously shown that enolase is increased in cytosolic samples in response to TCBZ-SO exposure [27] suggesting increased enolase abundance may be a general response to xenobiotic exposure. Indeed, work by Cornish and Bryant [44] observed an increase of energy metabolising products post stimulation with benzimidazole drugs further suggesting increased enolase abundance may be a general anthelmintic response.

Finally, four proteins, actin, gelsolin, DJ-1 and triose phosphate isomerise (Tpi), were identified as potential biomarkers of TCBZ-SO terminating fluke, rather than biomarkers of simply TCBZ-SO exposure. All of these proteins have been found previously associated with the tegument [42,43] and all, with the exception of DJ-1, have been identified in ES products [see 42]. Upon reductions in fluke viability, and ultimately death, more components associated with the tegument are released into ES products [21], an observation also seen in other flukes; both *S. haematobium* actin and Tpi revealed post PZQ treatment [32]. Therefore, these sub tegumental/tegumental associated proteins may become suitable markers for measuring the death of *F. hepatica*.

Fasciola Glutathione transferases (GST) are a recognised component of *in vitro* ES products. Both Sigma and Mu class GSTs have been identified in adult and juvenile ES products [43,45,46]. Interestingly, GSTs have also been implicated in the TCBZ-SO response in *F. hepatica*. In particular, Chemale et al. [27] identified a Mu class GST responding as a result of TCBZ-SO exposure and the study of Shehab et al. [47] observed greater levels of GST activity as a result of TCBZ-SO treatment. Despite these findings, no GSTs were identified in the current study. However, the two previous studies were investigating cytosolic responses and GSTs only contribute a small proportion to the total ES products.

An important consideration, in *in vitro* maintenance studies such as this, is the TCBZ-SO susceptibility/resistance status of the liver fluke used. In the current study, the liver fluke used were of 'wild-type' susceptibility. Thus, the two response profiles identified can relate to 'wild-type' susceptibility. Following on from the current study it will be prudent to assess the fingerprint response profiles of defined liver fluke TCBZ-SO resistant isolates. There is then the possibility to identify

a third subset of potential biomarkers – markers of TCBZ-SO resistance.

5. Conclusions

Two panels of *F. hepatica* proteins have been identified in the current study; TCBZ-SO survival markers (CRT, Cat L proteases and enolase) and confirmed TCBZ-SO killing markers (actin, gelsolin, DJ-1 and Tpi). Therefore, this study provides several new *F. hepatica* protein candidates for validation in diagnostic testing of TCBZ response (measuring drug failure or resistance). These new ES markers need to be confirmed as identifiable in infected host faeces, as either intact or fragmented proteins by antibody detection. This proteomic lead approach is transferable to other parasitic or microbial systems for the identification of biomarkers for antimicrobial/anthelmintic action.

Acknowledgements

This work was supported by Meat Promotion Wales (HCC), Quality Meat Scotland (QMS), EBLEX and the Welsh Assembly Government ESDF (Grant number HE 11 ESD 1005). The funders had no role in the design or completion of the current study. The authors are grateful to Randall Parker Foods (Wales) for providing *F. hepatica* infected sheep livers and Dr Hazel Wright (Farmers Union of Wales) for statistical advice. The authors would like to dedicate this work to the late Prof. John Barrett.

Appendix A. Supplementary data

Supplementary data associated with this article can be found, in the online version, at doi:10.1016/j.euprot.2014.02.013.

REFERENCES

[1] Boray JC. Chemotherapy of infections with fasciolidae. In: Boray JC, editor. Immunology, pathobiology and control of Fasciolosis. New Jersey: MSD AGVET Rahway; 1997. p. 83–97.
[2] Claridge J, Diggle P, McCann CM, Mulcahy G, Flynn R, McNair J, et al. *Fasciola hepatica* is associated with the failure to detect bovine tuberculosis in dairy cattle. Nat Commun 2012;3, http://dx.doi.org/10.1038/ncomms840.
[3] Anonymous. Control of foodborne trematode infections. Geneva: WHO; 1995. p. 165.
[4] Brennan GP, Fairweather I, Trudgett A, Hoey E, McCoy, McConville M, et al. Understanding triclabendazole resistance. Exp Mol Pathol 2007;82:104–9.
[5] Overend DJ, Bowen FL. Resistance of *Fasciola hepatica* to Triclabendazole. Aust Vet J 1995;72:275–6.
[6] Fairweather I. Triclabendazole: new skills to unravel an old(ish) enigma. J Helminthol 2005;79:227–34.
[7] Gordon DK, Roberts LCP, Lean N, Zadoks RN, Sargison ND, Skuce PJ. Identification of the rumen fluke, *Calicophoron daubneyi*, in GB livestock: possible implications for liver fluke diagnosis. Vet Parasitol 2013;195:65–71.
[8] Fairweather I. Triclabendazole progress report, 2005–2009: an advancement of learning? J Helminthol 2009;83:139–50.
[9] Halferty L, Brennan GP, Trudgett A, Hoey L, Fairweather I. Relative activity of triclabendazole metabolites against the liver fluke, *Fasciola hepatica*. Vet Parasitol 2009;159:126–38.
[10] Stitt AW, Fairweather I. *Fasciola hepatica*: tegumental surface changes in adult and juvenile flukes following treatment *in vitro* with the sulfoxide metabolite of triclabendazole (Fasinex). Parasitol Res 1993;79:529–36.
[11] Stitt AW, Fairweather I. The effect of the sulfoxide metabolite of triclabendazole (Fasinex) on the tegument of mature and immature stages of the liver fluke, *Fasciola hepatica*. Parasitology 1994;108:555–67.
[12] Stitt AW, Fairweather I. *Fasciola hepatica*: disruption of the vitelline cells in vitro by the sulphoxide metabolite of triclabendazole. Parasitol Res 1996;82:333–9.
[13] Hanna RE, Moffett D, Brennan GP, Fairweather I. *Fasciola hepatica*: a light and electron microscope study of sustentacular tissue and heterophagy in the testis. Vet Parasitol 2012;187:168–82.
[14] Stitt AW, Fairweather I, Mackender RO. The effect of triclabendazole (Fasinex) on protein synthesis by the liver fluke, *Fasciola hepatica*. Int J Parasitol 1995;25:421–9.
[15] Bennett JL, Kohler P. *Fasciola hepatica*: action *in vitro* of triclabendazole on immature and adult stages. Exp Parasitol 1987;63:49–57.
[16] Lanusse CE, Prichard RK. Clinical pharmacokinetics and metabolism of benzimidazole anthelmintics in ruminants. Drug Metab Rev 1993;25:235–79.
[17] Alvarez LI, Solana HD, Mottier ML, Virkel GL, Fairweather I, Lanusse CE. Altered drug influx/efflux and enhanced metabolic activity in triclabendazole-resistant liver flukes. Parasitology 2005;131:501–10.
[18] Virkel G, Lifschitz A, Sallovitz J, Pis A, Lanusse C. Assessment of the main metabolism pathways for the flukicidal compound triclabendazole in sheep. J Vet Pharmacol Ther 2006;29:213–23.
[19] Hennessy DR, Lacey E, Steel JW, Prichard RK. The kinetics of triclabendazole disposition in sheep. J Vet Pharmacol Ther 1987;10:64–72.
[20] Mezo M, Gonzalez-Warleta M, Carro C, Ubeira FM. An ultrasensitive capture ELISA for detection of *Fasciola hepatica* coproantigens in sheep and cattle using a new monoclonal antibody (MM3). J Parodontol 2004;90:845–52.
[21] Morphew RM, Wright HA, LaCourse EJ, Woods DJ, Brophy PM. Comparative proteomics of excretory-secretory proteins released by the liver fluke *Fasciola hepatica* in sheep host bile and during *in vitro* culture ex-host. Mol Cell Proteomics 2007;6:963–72.
[22] Brophy PM, Mackintosh N, Morphew RM. Anthelmintic metabolism in parasitic helminths: proteomic insights. Parasitology 2012;139:1205–17.
[23] Morphew RM, Wright HA, LaCourse EJ, Porter J, Barrett J, Woods DJ, et al. Towards delineating functions within the *Fasciola* secreted cathepsin L protease family by integrating *in vivo* based sub-proteomics and phylogenetics. PLoS Negl Trop Dis 2011;5:e937, http://dx.doi.org/10.1371/journal.pntd.0000937.
[24] Gorg A, Postel W, Weser J, Gunther S, Strahler JR, Hanash SM, et al. Elimination of point streaking on silver stained two-dimensional gels by addition of iodoacetamide to the equilibration buffer. Electrophoresis 1987;8:122–4.
[25] Breiman L. Random forests. Mach Learn 2001;45:5–32.
[26] Hart EH, Morphew RM, Bartley DJ, Millares P, Wolf BT, Brophy PM, et al. The soluble proteome phenotypes of ivermectin resistant and ivermectin susceptible *Haemonchus contortus* females compared. Vet Parasitol 2012;190:104–13.
[27] Chemale G, Perally S, LaCourse EJ, Prescott MC, Jones LM, Ward D, et al. Comparative proteomic analysis of triclabendazole response in the liver fluke *Fasciola hepatica*. J Proteome Res 2010;9:4940–51.

[28] Moxon JV, LaCourse EJ, Wright HA, Perally S, Prescott MC, Gillard JL, et al. Proteomic analysis of embryonic *Fasciola hepatica*: characterization and antigenic potential of a developmentally regulated heat shock protein. Vet Parasitol 2010;169:62–75.
[29] Kasper G, Brown A, Eberl M, Vallar L, Kieffer N, Berry C, et al. A calreticulin-like molecule from the human hookworm *Necator americanus* interacts with C1q and the cytoplasmic signalling domains of some integrins. Parasite Immunol 2001;23:141–52.
[30] Khalife J, Liu JL, Pierce R, Porchet E, Godin C, Capron A. Characterization and localization of *Schistosoma mansoni* calreticulin SM58. Parasitology 1994;108:527–32.
[31] Suchitra S, Joshi P. Characterization of *Haemonchus contortus* calreticulin suggests its role in feeding and immune evasion by the parasite. Biochim Biophys Acta 2005;1722:293–303.
[32] Mutapi F, Burchmore R, Mduluza T, Foucher A, Harcus Y, Nicoll G, et al. Praziquantel treatment of individuals exposed to *Schistosoma haematobium* enhances serological recognition of defined parasite antigens. J Infect Dis 2005;192:1108–18.
[33] Ferreira V, Molina MC, Valck C, Rojas A, Aguilar L, Ramirez G, et al. Role of calreticulin from parasites in its interaction with vertebrate hosts. Mol Immunol 2004;40:1279–91.
[34] Michalak M, Corbett EF, Mesaeli N, Nakamura K, Opas M. Calreticulin: one protein, one gene, many functions. Biochem J 1999;344:281–92.
[35] Greenberg RM. Ca^{2+} signalling, voltage-gated Ca^{2+} channels and praziquantel in flatworm neuromusculature. Parasitology 2005;131:S97–108.
[36] Mery L, Mesaeli N, Michalak M, Opas M, Lew DP, Krause KH. Overexpression of calreticulin increases intracellular Ca^{2+} storage and decreases store-operated Ca^{2+} influx. J Biol Chem 1996;271:9332–9.
[37] Michalak M, Groenendyk J, Szabo E, Gold LI, Opas M. Calreticulin, a multi-process calcium-buffering chaperone of the endoplasmic reticulum. Biochem J 2009;417:651–66.
[38] Xu KL, Tavernarakis N, Driscoll M. Necrotic cell death in *C. elegans* requires the function of calreticulin and regulators of Ca^{2+} release from the endoplasmic reticulum. Neuron 2001;31:957–71.
[39] Robinson MW, Tort JF, Lowther J, Donnelly SM, Wong E, Xu W, et al. Proteomic and phylogenetic analysis of the cathepsin L protease family of the helminth pathogen, *Fasciola hepatica*: expansion of a repertoire of virulence-associated factors. Mol Cell Proteomics 2008;7:1111–23.
[40] Rhoads ML, Fetterer RH. Developmentally-regulated secretion of cathepsin L-like cysteine proteases by *Haemonchus contortus*. J Parasitol 1995;81:505–12.
[41] Bernal D, de la Rubia JE, Carrasco-Abad AM, Toledo R, Mas-Coma S, Marcilla A. Identification of enolase as a plasminogen-binding protein in excretory-secretory products of *Fasciola hepatica*. FEBS Lett 2004;563:203–6.
[42] Morphew RM, Hamilton CM, Wright HA, Dowling DJ, O'Neill SM, Brophy PM. Identification of the major proteins of an immune modulating fraction from adult *Fasciola hepatica* released by Nonidet P40. Vet Parasitol 2012;191:379–85.
[43] Wilson RA, Wright JM, de Castro-Borges W, Parker-Manuel SJ, Dowle AA, Ashton PD, et al. Exploring the *Fasciola hepatica* tegument proteome. Int J Parasitol 2011;41:1347–59.
[44] Cornish RA, Bryant C. Changes in energy-metabolism due to anthelmintics in *Fasciola hepatica* maintained *in vitro*. Int J Parasitol 1976;6:393–8.
[45] LaCourse JE, Perally S, Morphew RM, Moxon JV, Prescott MC, Dowling D, et al. The sigma class glutathione transferase of the liver fluke *Fasciola hepatica*. PLoS Negl Trop Dis 2012;5:e937, http://dx.doi.org/10.1371/journal.pntd.0000937.
[46] Morphew RM, Eccleston N, Wilkinson TJ, McGarry J, Perally S, Prescott M, et al. Proteomics and *in silico* approaches to extend understanding of the glutathione transferase superfamily of the tropical liver fluke *Fasciola gigantica*. J Proteome Res 2012;11:5876–89.
[47] Shehab AY, Ebeid SM, El-Samak MY, Hussein NM. Detoxifying and anti-oxidant enzymes of *Fasciola gigantica* worms under triclabendazole sulphoxide (TCBZ-SX): an *in vitro* study. J Egypt Soc Parasitol 2009;39:73–83.